Rate-dependent Thermo-mechanical Modelling of Superelastic Shape-memory Alloys for Seismic Applications

FERDINANDO AURICCHIO,[1,2,3] DAVIDE FUGAZZA[1,3,*] AND REGINALD DESROCHES[4]

[1]*Dipartimento di Meccanica Strutturale, Università degli Studi di Pavia*
Via Ferrata 1, 27100 Pavia, Italy

[2]*Istituto di Matematica Applicata e Tecnologie Informatiche, Università degli Studi di Pavia*
Via Ferrata 1, 27100 Pavia, Italy

[3]*European School for Advanced Studies in Reduction of Seismic Risk (ROSE School)*
Via Ferrata 1, 27100 Pavia, Italy

[4]*School of Civil and Environmental Engineering, Georgia Institute of Technology*
790 Atlantic Drive, Atlanta, GA 30332-0355, USA

ABSTRACT: Experimental tests performed on superelastic shape-memory alloys (SMAs) show a significant dependence of the stress–strain relationship on the loading–unloading rate, coupled with a not negligible oscillation of the material temperature. This feature is of particular importance in view of the use of such materials in earthquake engineering, where the loading rate affects the structural response. Motivated by this observation and by the limited number of available works on the modelling of SMAs for seismic applications, the present article addresses a uniaxial constitutive model for representing the system rate-dependent thermo-mechanical behavior of superelastic SMAs. The model is based on a single internal scalar variable, the martensite fraction, for which different rate-independent evolutionary equations in rate form are proposed. Moreover, it takes into account the different elastic properties between austenite and martensite. The whole model is then thermo-mechanically coupled with a thermal balance equation. Hence, it considers mechanical dissipation as well as latent heat and includes temperature as a primary independent variable, which is responsible for the dynamic effects. The article also provides a description for the integration, in time, of the constitutive equation and presents the solution algorithm of the corresponding time-discrete problem. Finally, results from numerical analyses are reported and the ability of the model to simulate experimental data obtained from uniaxial tests performed on superelastic SMA wires and bars at frequency levels of excitation typical of earthquake engineering is assessed.

Key Words: shape-memory alloys, constitutive modelling, experimental tests, seismic applications.

INTRODUCTION

SHAPE-MEMORY alloys (SMAs) are a class of solids with an intrinsic ability to remember an original shape. This particular mechanical behavior relies on reversible micromechanical phase transitions taking place during deformation and/or temperature processes, when the SMAs' crystallographic structure switches from an austenitic phase to a martensitic phase.

At the macroscopic level, SMAs feature two uncommon properties not possessed by traditional materials utilized in engineering. They are the superelastic effect and the shape-memory effect. The first is related to the ability of the material to regain, under certain temperature conditions, its initial configuration upon removal of the external load and, the second, is the capacity of the alloy to go back to its undeformed shape by means of thermal cycles (Duerig et al., 1990).

Due to these unique characteristics, SMAs have had a strong impact in today's market with the production of numerous innovative devices. To name a few, it is worth recalling biomedical prostheses, eyeglass frames, cellular phone antennas and apparatus for the deployment and control of space structures.

Recent experimental and numerical investigations have also shown the possibility of using such materials in the area of seismic resistant design and retrofit.

*Author to whom correspondence should be addressed. Currently at SAMTECH Italia, Via Giovanni Rasori 13, 20145 Milano, Italy.
E-mail: davide.fugazza@samcef.com
Figures 1–13 appear in color online: http://jim.sagepub.com

1045-389X/08/01 0047–15 $10.00/0 DOI: 10.1177/1045389X06073426

In particular, they have been shown to be effective in improving the response of buildings and bridges subjected to earthquake-induced vibrations (Saadat et al., 2002; DesRoches and Smith, 2004; Wilson and Wesolosky, 2005).

Despite the large number of constitutive equations available in the literature, few studies deal with the material modelling of SMAs under dynamic loadings, and, specifically, for applications in earthquake engineering.

In this respect, the present work proposes a uniaxial constitutive equation able to describe the system rate-dependent superelastic behavior of such materials. The model is based on a single internal scalar variable, the martensite fraction, for which three different rate-independent evolutionary equations in rate form are proposed. Moreover, it is able to describe the different elastic properties between austenite and martensite.

The whole model is then coupled with a thermal balance equation, due to the presence of internal heat sources in the form of phase-transition latent heat and mechanical dissipation. It also considers the temperature as a primary independent variable, which is responsible for its rate-dependent nature. Finally, after discussing the integration technique for the solution of the corresponding time-discrete framework and after showing some numerical tests aimed at evaluating its performance, the ability of the model to reproduce experimental data obtained from uniaxial tests performed on superelastic SMA wires and bars of different size and chemical composition at frequency levels of excitation typical of earthquake engineering is assessed.

CONSTITUTIVE MODELLING OF SMAs FOR SEISMIC APPLICATIONS

In this section, we focus attention on the constitutive modelling of superelastic SMAs by reviewing the material laws that have been used for describing the response of SMA-based devices for seismic applications. Since such devices are traditionally used in earthquake engineering as a combination of wires or bars (Saadat et al., 2002; DesRoches and Smith, 2004; Wilson and Wesolowsky, 2005), emphasis is given only to uniaxial models.

Graesser and Cozzarelli (1991) took into consideration the possibility of using SMAs for seismic applications and proposed an equation able to capture both the superelastic effect and the martensitic hysteresis. Drawbacks of the formulation were the inability to predict the material behavior after phase transition completion as well as both the rate- and temperature-independence.

Bernardini and Brancaleoni (1999) focused on a constitutive law able to simulate the rate- and temperature-dependent response of SMAs, with the aim of predicting the dynamic response of frames equipped with SMA-based devices undergoing seismic excitations. In the proposed equation, SMAs were represented as a mixture of two solid phases whose individual behavior was modeled as a linear isotropic thermoelastic material.

Wilde et al. (2000) proposed an innovative device made of SMA bars for bridge isolation. They improved the Graesser and Cozzarelli model by describing the material behavior after phase transformation completion. However, the model was still rate- and temperature-independent.

Tamai and Kitagawa (2002) considered a temperature-dependent model in which the phase transformation stress levels were depending on the martensite fraction. The adopted kinetic rules were exponential and differed according to the phase transformation being considered. However, the constitutive law was rate-independent and required a large number of experimental data. The model was used for evaluating the seismic response of SMA elements.

From the above summary on the modelling approach of SMAs for seismic applications, it is clear that the dependence of the material on the loading–unloading rate is, in general, not taken into consideration.

Furthermore, since energetic considerations and temperature changes play a major role in the phase transformations underlying the superelastic response of SMAs (Shaw and Kyriakides, 1995; Shaw and Kyriakides, 1997; Entemeyer et al., 2000; Müller and Seelecke, 2001; Anand and Gurtin, 2003; Brinson et al., 2004), there is a strong need for a thermomechanical model able to reproduce such a feature. Accordingly, the present article would like to explore a possible path to include such an effect in the proposed model and make comparisons with experimental data.

TIME-CONTINUOUS MODEL

We now present a uniaxial thermo-mechanical time-continuous phenomenological constitutive model for superelastic SMAs, developed within the theory of irreversible thermodynamics (Auricchio and Sacco, 2001) and the general internal variable framework (Lubliner and Auricchio, 1996). Its most important features, that will be discussed in the next sections, are listed as follows:

- Simplicity and complete soundness in a thermodynamic framework.
- Ability to describe a number of rate-dependent superelastic behaviors by considering three different kinetic rules.
- Possibility of implementing a robust solution algorithm for the integration of the constitutive law.

- Ability to reproduce experimental data related to SMA elements tested in both quasi-static and dynamic loading conditions.

General Framework

We assume that at each time instant the thermodynamic state of a volume element is characterized by a set of external and internal variables. More precisely, we choose as external variables the uniaxial strain, ϵ, and the absolute temperature, T, and as internal variable a scalar quantity, ξ, representing the volume of martensite fraction.

A necessary ingredient will then be the free energy, named as ψ, depending on both internal and external variables.

Evolution of Elastic Modulus

Experimental tests show large differences between the elastic properties of austenite and martensite (Dolce and Cardone, 2001; DesRoches et al., 2004; Fugazza, 2005). To model this aspect, we assume the elastic modulus to be a function of the martensite fraction by requiring that:

$$E(\xi = 0) = E_{\mathrm{A}} \qquad \text{and} \qquad E(\xi = 1) = E_{\mathrm{M}} \tag{1}$$

being E_{A} and E_{M} the elastic modulus of austenite and martensite, respectively. Valid expressions for E can be obtained by regarding the SMA as a material made of a volume fraction of austenite and a volume fraction of martensite. Then, the overall elastic properties of the composite can be recovered through the well-known homogenization theory.

Addressing the reader to more specific works dealing with such a topic, and following Auricchio and Sacco (1997) as well as Ikeda et al. (2004), for the specific problem being investigated (i.e., uniaxial state of stress of SMA wires and bars subjected to cyclic loadings) we adopt the Reuss scheme. In particular, knowing the values E_{A}, E_{M} and the martensite fraction, ξ, the overall equivalent elastic modulus is given by:

$$E = \frac{E_{\mathrm{A}}\, E_{\mathrm{M}}}{E_{\mathrm{M}} + (E_{\mathrm{A}} - E_{\mathrm{M}})\,\xi}. \tag{2}$$

With such assumption, which experimental investigation confirmed to be realistic, we consider the SMA material as an austenite–martensite periodic composite in which the total elongation of its periodic cell undergoing uniaxial loads is given by the sum of the elongation of the austenitic part and the martensitic part. These parts, from a mechanical point of view, are seen as two springs of different elastic properties acting in series. Finally, Equation (2) gives a lower bound for the overall elastic modulus of the considered SMA material.

Strain Decomposition

Limiting the discussion to a small deformation regime, we assume an additive decomposition of the total strain, ϵ, of the form:

$$\epsilon = \epsilon^{\mathrm{el}} + \epsilon^{\mathrm{in}} \tag{3}$$

where

- ϵ^{el} represents the thermo-elastic strain and, by definition, it depends only on the control variables and it includes contributions such as the pure elastic term as well as the thermo-elastic expansion term.
- ϵ^{in} represents the inelastic strain, which may depend also on the set of internal variables, that is, in the present case, the martensite fraction ξ.

In particular, we express the inelastic strain as:

$$\epsilon^{\mathrm{in}} = \epsilon_L\, \xi\, \mathrm{sgn}(\sigma) \tag{4}$$

where

- ϵ_L is a measure of the maximum deformation obtainable by aligning the martensite in one direction and in the following considered as a material parameter.
- sgn is the sign function defined as:

$$\mathrm{sgn}(x) = \begin{cases} -1 & \text{if } x < 0 \\ 0 & \text{if } x = 0 \\ +1 & \text{if } x > 0. \end{cases} \tag{5}$$

- σ is the uniaxial stress.

Free Energy and Stress Definition

On the basis of the work by Auricchio and Sacco (2001), we consider the following free energy:

$$\begin{aligned} \psi = {} & [(u_{\mathrm{A}} - T\eta_{\mathrm{A}}) - \xi(\Delta u - T\Delta\eta)] \\ & + C\left[(T - T_0) - T\log\frac{T}{T_0}\right] + \frac{1}{2}\, E\,[\epsilon - \epsilon_L\, \xi\, \mathrm{sgn}(\sigma)]^2 \\ & - (T - T_0)[\epsilon - \epsilon_L\, \xi\, \mathrm{sgn}(\sigma)]E\alpha \end{aligned} \tag{6}$$

where

- u_{A} and η_{A} are the internal energy and the entropy of the austenite,
- Δu and $\Delta\eta$ are the internal energy difference and the entropy difference between the austenite and the martensite. In particular, we set

$$\Delta u = u_{\mathrm{A}} - u_{\mathrm{M}} \geq 0 \qquad \text{and} \qquad \Delta\eta = \eta_{\mathrm{A}} - \eta_{\mathrm{M}} \geq 0 \tag{7}$$

with u_{M} and η_{M} the internal energy and the entropy of the martensite.

- C is the material heat capacity,
- T_0 is the natural or reference state temperature,
- α is the thermal expansion factor.

Accordingly, the stress is defined as:

$$\sigma = \frac{\partial \psi}{\partial \epsilon} = E[\epsilon - \epsilon_L \xi \operatorname{sgn}(\sigma)] - E\alpha(T - T_0). \quad (8)$$

Furthermore, by recalling the definition of ϵ^{el} and by considering Equation (4), we can observe that there is a linear relationship between stress and elastic strain:

$$\sigma = E\epsilon^{\mathrm{el}}. \quad (9)$$

Finally, introduction of Equations (4) and (9) into Equation (3) indicates that $\operatorname{sgn}(\sigma) = \operatorname{sgn}(\epsilon)$. This last equality will be particularly useful during the development of the solution algorithm.

Heat Equation

According to the classical literature (Lemaitre and Chaboche, 1990), the heat equation can be written as:

$$C\dot{T} + \operatorname{div}\mathbf{q} = b - \gamma(T - T_{\mathrm{ext}}) \quad (10)$$

where div indicates the divergence operator, a superposed dot indicates a time-derivative, $\mathbf{q}$ is the heat flux, b is the heat source, and γ the heat convection coefficient which governs the interaction between the material and the surrounding environment.[1] Such a parameter is, in general, very difficult to determine as it depends on a number of variables such as material temperature and shape of the specimen. Since for this specific study we are considering elements with small size cross sections (i.e., wires and bars), in the previous equation we may neglect the contribution given by the heat flux. Accordingly:

$$C\dot{T} = b - \gamma(T - T_{\mathrm{ext}}) \quad (11)$$

with the heat source (Leclercq and Lexcellent, 1996; Entemeyer et al., 2000; Auricchio and Sacco, 2001; Bernardini and Pence, 2002; Lim and McDowell, 2002; Anand and Gurtin, 2003) that can be described as the sum of two contributions:

$$b = \mathcal{H}_{\mathrm{tmc}} + \mathcal{D}_{\mathrm{mec}} \quad (12)$$

where

- $\mathcal{H}_{\mathrm{tmc}}$ represents the heat production associated to the thermo-mechanical coupling and it is defined as:

$$\mathcal{H}_{\mathrm{tmc}} = T\frac{\partial^2 \psi}{\partial T \partial \epsilon}\dot{\epsilon} + T\frac{\partial^2 \psi}{\partial T \partial \xi}\dot{\xi} \quad (13)$$

- $\mathcal{D}_{\mathrm{mec}}$ represents the heat production associated to the dissipative mechanical processes and it is defined as:

$$\mathcal{D}_{\mathrm{mec}} = \sigma\dot{\epsilon} - \left(\frac{\partial \psi}{\partial \epsilon}\dot{\epsilon} + \frac{\partial \psi}{\partial \xi}\dot{\xi}\right). \quad (14)$$

We recall that the mechanical dissipation is in general required to be non-negative: $\mathcal{D}_{\mathrm{mec}} \geq 0$. The last expression is well known as Clausius–Duhem inequality and comes from the second law of thermodynamics.

Due to the specific form of free energy chosen, we have:

$$\mathcal{H}_{\mathrm{tmc}} = T\{-E\alpha\dot{\epsilon} + [\Delta\eta + E\alpha\epsilon_L \operatorname{sgn}(\sigma)]\dot{\xi}\} \quad (15)$$

$$\mathcal{D}_{\mathrm{mec}} = \Pi\dot{\xi} \quad (16)$$

with

$$\Pi = \Delta u - T\Delta\eta + \epsilon_L|\sigma| \quad (17)$$

modelling the thermodynamic force associated to ξ.

Kinetic Rules

We assume to work with two processes which may produce variations of the martensite fraction:

- the conversion of austenite into martensite (A $\rightarrow$ M),
- the conversion of martensite into austenite (M $\rightarrow$ A).

For each process, we can observe (Auricchio and Sacco, 2001) that the driving force can be expressed as:

$$F = |\sigma| - T\Omega \quad (18)$$

where

$$\Omega = \frac{\Delta\eta}{\epsilon_L} \quad (19)$$

consistently, with experimental evidences showing that both processes can be either stress and/or temperature driven (Duerig et al., 1990) and that they may occur in stress–temperature regions delimited, with good approximations, by straight lines whose slope is given by the term Ω previously introduced (Figure 1).

Starting from Auricchio and Sacco (1999b) and Auricchio and Sacco (2001) and using the same terminology introduced by Auricchio (1995), we consider different kinetic rules, linear, power, and exponential, in the following presented according to an increasing order of complexity. They represent the evolution in time of the martensite fraction and are expressed through first-order differential equations.

[1] It is worth recalling that the material temperature increases and decreases during the deformation process due to the heat convection between the material and the surrounding environment, the latent heat and the dissipation energy due to internal friction.

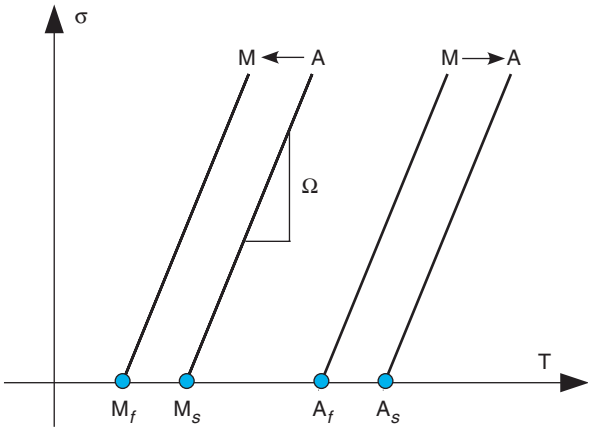

Figure 1. *Phase transformation zones (A = austenite, M = martensite, Ω = slope). A_s, A_f, M_s, and M_f are the temperature levels at which the forward (A → M) and reverse (M → A) phase transformation starts and finishes, respectively.*

CONVERSION OF AUSTENITE INTO MARTENSITE

$$\text{Linear} \quad \dot{\xi} = -(1-\xi)\,\frac{\dot{F}}{F - R_f^{\mathrm{AM}}}\,\mathcal{H}^{\mathrm{AM}}$$

$$\text{Power} \quad \dot{\xi} = -\pi^{\mathrm{AM}}(1-\xi)\,\frac{\dot{F}}{F - R_f^{\mathrm{AM}}}\,\mathcal{H}^{\mathrm{AM}}$$

$$\text{Exponential} \quad \dot{\xi} = \beta^{\mathrm{AM}}(1-\xi)\,\frac{\dot{F}}{(F - R_f^{\mathrm{AM}})^2}\,\mathcal{H}^{\mathrm{AM}}. \tag{20}$$

The term $\mathcal{H}^{\mathrm{AM}}$ is the activation factor relative to the A → M transformation and it is defined as:

$$\mathcal{H}^{\mathrm{AM}} = \begin{cases} 1 & \text{when } \dot{F} > 0 \text{ and } R_s^{\mathrm{AM}} < F < R_f^{\mathrm{AM}} \\ 0 & \text{otherwise} \end{cases} \tag{21}$$

where

$$R_s^{\mathrm{AM}} = \sigma_s^{\mathrm{AM}} - T_R\,\Omega \qquad R_f^{\mathrm{AM}} = \sigma_f^{\mathrm{AM}} - T_R\,\Omega \tag{22}$$

The quantities σ_s^{AM} and σ_f^{AM} are material properties representing, respectively, the stress level at which the A → M transformation starts and finishes at temperature T_R. Also, coefficients π^{AM} and β^{AM} represent the speed parameters modelling the considered phase transformation.

CONVERSION OF MARTENSITE INTO AUSTENITE

$$\text{Linear} \quad \dot{\xi} = \xi\,\frac{\dot{F}}{F - R_f^{\mathrm{MA}}}\,\mathcal{H}^{\mathrm{MA}}$$

$$\text{Power} \quad \dot{\xi} = \pi^{\mathrm{MA}}\,\xi\,\frac{\dot{F}}{F - R_f^{\mathrm{MA}}}\,\mathcal{H}^{\mathrm{MA}} \tag{23}$$

$$\text{Exponential} \quad \dot{\xi} = \beta^{\mathrm{MA}}\,\xi\,\frac{\dot{F}}{(F - R_f^{\mathrm{MA}})^2}\,\mathcal{H}^{\mathrm{MA}}.$$

The term $\mathcal{H}^{\mathrm{MA}}$ is the activation factor relative to the M → A transformation and it is defined as:

$$\mathcal{H}^{\mathrm{MA}} = \begin{cases} 1 & \text{when } \dot{F} < 0 \text{ and } R_f^{\mathrm{MA}} < F < R_s^{\mathrm{MA}} \\ 0 & \text{otherwise} \end{cases} \tag{24}$$

where

$$R_s^{\mathrm{MA}} = \sigma_s^{\mathrm{MA}} - T_R\,\Omega \qquad R_f^{\mathrm{MA}} = \sigma_f^{\mathrm{MA}} - T_R\,\Omega. \tag{25}$$

The quantities σ_s^{MA} and σ_f^{MA} are material properties representing, respectively, the stress level at which the M → A transformation starts and finishes at temperature T_R. Also, coefficients π^{MA} and β^{MA} represent the speed parameters modelling the considered phase transformation.

Remark. To guarantee the non-negativeness of the mechanical dissipation $\mathcal{D}_{\mathrm{mec}}$, the mechanical parameters σ_s^{AM}, σ_f^{AM}, σ_s^{MA} and σ_f^{MA} should verify the following inequalities:

$$\begin{aligned} \sigma_R &\le \sigma_s^{\mathrm{AM}} \le \sigma_f^{\mathrm{AM}} \\ \sigma_s^{\mathrm{MA}} &\le \sigma_s^{\mathrm{MA}} \le \sigma_R \end{aligned} \tag{26}$$

where σ_R is computed from the condition $\Pi = 0$ for $T = T_R$. As a consequence:

$$\sigma_R = \frac{T_R\,\Delta\eta - \Delta u}{\epsilon_L}. \tag{27}$$

TIME-DISCRETE MODEL AND ALGORITHMIC SOLUTION

The time-discrete model is obtained by integrating the time-continuous model over the time-interval $[t_n, t]$ through a backward-Euler integration scheme as discussed in the following. To minimize the appearance of subscripts, the subscript n indicates a quantity that is evaluated at time t_n, while no subscript indicates a quantity that is evaluated at time t, with $t_n < t$.

Integration of Heat Equation

Integration of the heat equation leads to:

$$C\,\frac{T - T_n}{t - t_n} - b_d + \gamma\,(T - T_{\mathrm{ext}}) = 0 \tag{28}$$

where

$$b_d = \frac{1}{t - t_n}\,[\Pi\,\lambda + T\,\Gamma] \tag{29}$$

with

$$\lambda = \xi - \xi_n \tag{30}$$

$$\Pi = \Delta u - T\Delta\eta + \epsilon_L|\sigma| \tag{31}$$

$$\Gamma = -E\,\alpha\,(\epsilon - \epsilon_n) + [E\,\epsilon_L\,\alpha\,\mathrm{sgn}(\sigma) + \Delta\eta]\,\lambda \tag{32}$$

and with ϵ and ϵ_n assumed to be always known.

Integration of Kinetic Rules

We can instead obtain the time-discrete phase-transition rules by writing Equations (20) and (23) in residual form. After clearing the fractions, we get the following algebraic expressions.

CONVERSION OF AUSTENITE INTO MARTENSITE

$$\begin{aligned}
\text{Linear}\quad & \mathcal{R}^{\mathrm{AM}} = \lambda\left(F - R_f^{\mathrm{AM}}\right) \\
& \quad + (1-\xi)(F-F_n)\mathcal{H}^{\mathrm{AM}} = 0 \\
\text{Power}\quad & \mathcal{R}^{\mathrm{AM}} = \lambda\left(F - R_f^{\mathrm{AM}}\right) \\
& \quad + \pi^{\mathrm{AM}}(1-\xi)(F-F_n)\mathcal{H}^{\mathrm{AM}} = 0 \\
\text{Exponential}\quad & \mathcal{R}^{\mathrm{AM}} = \lambda\left(F - R_f^{\mathrm{AM}}\right)^2 \\
& \quad - \beta^{\mathrm{AM}}(1-\xi)(F-F_n)\mathcal{H}^{\mathrm{AM}} = 0. \qquad (33)
\end{aligned}$$

CONVERSION OF MARTENSITE INTO AUSTENITE

$$\begin{aligned}
\text{Linear}\quad & \mathcal{R}^{\mathrm{MA}} = \lambda\left(F - R_f^{\mathrm{MA}}\right) - \xi(F-F_n)\mathcal{H}^{\mathrm{MA}} = 0 \\
\text{Power}\quad & \mathcal{R}^{\mathrm{MA}} = \lambda\left(F - R_f^{\mathrm{MA}}\right) - \pi^{\mathrm{MA}}\xi(F-F_n)\mathcal{H}^{\mathrm{MA}} = 0 \\
\text{Exponential}\quad & \mathcal{R}^{\mathrm{MA}} = \lambda\left(F - R_f^{\mathrm{MA}}\right)^2 - \beta^{\mathrm{MA}}\xi(F-F_n)\mathcal{H}^{\mathrm{MA}} = 0. \qquad (34)
\end{aligned}$$

Equations (33) and (34) can be solved by means of an iterative strategy (i) or, when $\alpha = 0$, in closed-form (ii), as explained below.

(i) *Solution by iterative strategy*. As an iterative strategy, we select the Newton–Raphson scheme. To preserve its quadratic convergence, the derivatives of the time-discrete evolutionary equations written in residual form would be required in order to obtain the tangent modulus consistent with the time-discrete model. Since the computation needs long algebra, we do not include them in the article.

(ii) *Solution in closed form*. In the specific case in which $\alpha = 0$, substitution of Equation (36) into the time-discrete evolutionary equations written in residual form returns expressions of the type:

$$\begin{aligned}
C_2\,\xi^2 + C_1\,\xi + C_0 = 0 \qquad & \text{or} \\
C_3\,\xi^3 + C_2\,\xi^2 + C_1\,\xi + C_0 = 0 \qquad & (35)
\end{aligned}$$

whose roots can be found in closed-form. In particular, we obtain a quadratic expression for both linear and power rules and a cubic expression when considering the exponential rules. Due to the complexity of the coefficients, which are reported in Appendix 1, it seems impossible to perform a discussion of the roots of each equation. As a consequence, the admissible root is chosen as the one which is bounded between 0 (phase transformation not started yet) and 1 (complete phase transformation).

In order to improve the robustness of the solution procedure, we introduce two modifications to the model.

1. We scale the phase transition driving force, F, with respect to a temperature upper limit value T_{U}. Accordingly, its new expression becomes:
$$F = |\sigma| - (T - T_{\mathrm{U}})\,\Omega \qquad (36)$$
where T_{U} is an arbitrary temperature value such that $T < T_{\mathrm{U}}$. By means of Equation (36), we then guarantee the constant sign of F.
2. Following the considerations of Auricchio and Sacco (1999b) and Auricchio and Sacco (2001), we convert the activation factors as to be strain-controlled. In particular, they specialize to:

$$\mathcal{H}^{\mathrm{AM}} = \begin{cases} 1 & \text{when } \dot{G} > 0 \text{ and } S_s^{\mathrm{AM}} < G < S_f^{\mathrm{AM}} \\ 0 & \text{otherwise} \end{cases} \qquad (37)$$

$$\mathcal{H}^{\mathrm{MA}} = \begin{cases} 1 & \text{when } \dot{G} < 0 \text{ and } S_f^{\mathrm{MA}} < G < S_s^{\mathrm{MA}} \\ 0 & \text{otherwise} \end{cases} \qquad (38)$$

with

$$G = |\epsilon| - \frac{\Omega}{E}\,(T - T_{\mathrm{U}}) \qquad (39)$$

and

$$S_s^{\mathrm{AM}} = \frac{\sigma_s^{\mathrm{AM}}}{E} + \epsilon_L\,\xi_n \quad S_f^{\mathrm{AM}} = \frac{\sigma_s^{\mathrm{AM}}}{E} + \epsilon_L \qquad (40)$$

$$S_s^{\mathrm{MA}} = \frac{\sigma_s^{\mathrm{MA}}}{E} + \epsilon_L\,\xi_n \quad S_f^{\mathrm{MA}} = \frac{\sigma_f^{\mathrm{MA}}}{E}. \qquad (41)$$

Finally, in view of the computer implementation of the constitutive model, in Table 1 we summarize the main steps concerning the solution procedure and in Tables 2 and 3 we provide the solution schemes related to the two transformation processes.

NUMERICAL EXAMPLES

We now investigate the ability of the model to simulate the rate-dependent thermo-mechanical stress–strain response of a superelastic SMA material. We consider two different numerical tests:

- *Test* 1: Simple strain-driven loading–unloading cycle performed in quasi-static conditions up to 7% strain. The goal of this test is to understand the role of the speed parameters (i.e., π's and β's) that both power and exponential rules contain.

Table 1. Overall solution algorithm.

1. Compute G and G_n

$$G = |\epsilon| + \frac{\Omega}{E}(T - T_{\mathrm{U}})$$
$$G_n = |\epsilon_n| + \frac{\Omega}{E}(T_n - T_{\mathrm{U}})$$

2. Detect loading or unloading

if $|G - G_n| > 0 \Rightarrow$ loading
if $|G - G_n| < 0 \Rightarrow$ unloading

3. Check phase transformation

if loading then
  check A $\rightarrow$ M phase transformation (Table 2)
else if unloading then
  check M $\rightarrow$ A phase transformation (Table 3)
end if

4. Solve evolutionary equations

5. Solve heat equation

6. Compute stress

Table 2. Solution scheme for A $\rightarrow$ M phase transformation.

if $|G - G_n| > 0$ then $\Rightarrow$ loading

$$\epsilon_s^{\mathrm{AM}} = \mathrm{sgn}(\epsilon)\frac{R_s^{\mathrm{AM}}}{E} + \mathrm{sgn}(\epsilon)\xi_n \epsilon_L$$

$$\epsilon_f^{\mathrm{AM}} = \mathrm{sgn}(\epsilon)\frac{R_f^{\mathrm{AM}}}{E} + \mathrm{sgn}(\epsilon)\,\epsilon_L$$

if $|G - G_n| \le \epsilon_s^{\mathrm{AM}}$

$\xi = \xi_n$

$E = E_n$

else if $|G - G_n| > \epsilon_s^{\mathrm{AM}}$ and $|G - G_n| < \epsilon_f^{AM}$

Solve $\mathcal{R}^{\mathrm{AM}} = 0$ { Iterative strategy / Closed-form solution (if $\alpha = 0$)

$$E = \frac{E_{\mathrm{A}} E_{\mathrm{M}}}{E_{\mathrm{M}} + \xi(E_{\mathrm{A}} - E_{\mathrm{M}})}$$

else

$\xi = 1$

$E = E_{\mathrm{M}}$

end

end if

Table 3. Solution scheme for M $\rightarrow$ A phase transformation.

if $|G - G_n| < 0$ then $\Rightarrow$ unloading

$$\epsilon_s^{\mathrm{MA}} = \mathrm{sgn}(\epsilon)\frac{R_s^{\mathrm{MA}}}{E} + \mathrm{sgn}(\epsilon)\xi_n \epsilon_L$$

$$\epsilon_f^{\mathrm{MA}} = \mathrm{sgn}(\epsilon)\frac{R_f^{\mathrm{MA}}}{E}$$

if $|G - G_n| \ge \epsilon_s^{\mathrm{MA}}$

$\xi = \xi_n$

$E = E_n$

else if $|G - G_n| < \epsilon_s^{\mathrm{MA}}$ and $|G - G_n| > \epsilon_f^{MA}$

Solve $\mathcal{R}^{\mathrm{MA}} = 0$ { Iterative strategy / Closed-form solution (if $\alpha = 0$)

$$E = \frac{E_{\mathrm{A}} E_{\mathrm{M}}}{E_{\mathrm{M}} + \xi(E_{\mathrm{A}} - E_{\mathrm{M}})}$$

else

$\xi = 0$

$E = E_{\mathrm{A}}$

end

end if

- *Test* 2: Simple strain-driven loading–unloading cycle performed initially in 10^3 s and then, in a subsequent simulation, in 10^{-3} s in order to reproduce, respectively, very slow and very fast loading-unloading conditions. As in the previous test, the maximum strain attained is 7%. With this way of proceeding, we keep the same type of loading–unloading history while changing only the strain-rate at which it is applied (Auricchio and Sacco, 1999a). The goal of this test is to study the rate-dependent response of the model under investigation.

We consider material parameters[2] that are typical for commercial SMAs. More precisely, we choose:

$$E_{\mathrm{A}} = 40000\,\mathrm{MPa} \quad E_{\mathrm{M}} = 20000\,\mathrm{MPa} \quad \epsilon_L = 4.5\%$$
$$\sigma_s^{\mathrm{AM}} = 200\,\mathrm{MPa} \quad \sigma_f^{\mathrm{AM}} = 300\,\mathrm{MPa}$$
$$\sigma_s^{\mathrm{MA}} = 200\,\mathrm{MPa} \quad \sigma_f^{\mathrm{MA}} = 100\,\mathrm{MPa}$$
$$\Delta u = 30\,\mathrm{MPa} \quad \Delta\eta = 0.20\,\mathrm{MPaK}^{-1}$$
$$\alpha = 0\,\mathrm{K}^{-1} \quad \gamma = 0.1$$
$$C = 4\,\mathrm{MPaK}^{-1} \quad T_{\mathrm{ext}} = T_0 = T_R = 293\,\mathrm{K}$$
$$T_{\mathrm{U}} = 573\,\mathrm{K}.$$

Model Characteristics

In this section, we briefly summarize the main findings coming out from the numerical simulations, addressing the reader to the work by Auricchio et al. (2006) for further details.

[2]Since thermodynamic parameters were not identified experimentally, they have been chosen to be the same as the ones considered by Auricchio and Sacco (2001).

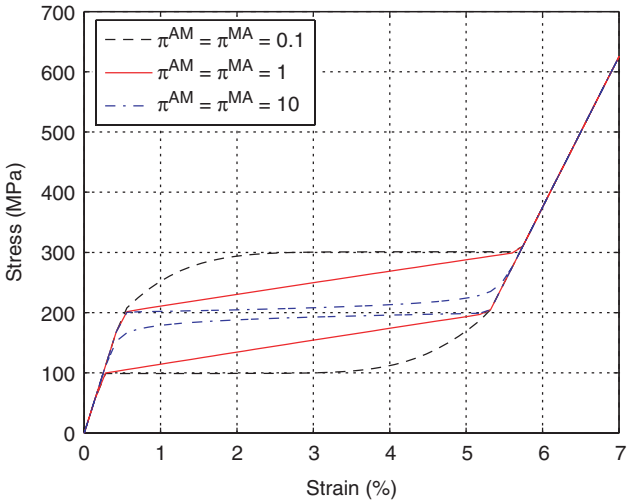

Figure 2. *Power rules: stress–strain relationship for quasi-static loading–unloading conditions. Setting speed parameters π^{AM} and π^{MA} equal to 1 leads to linear rules.*

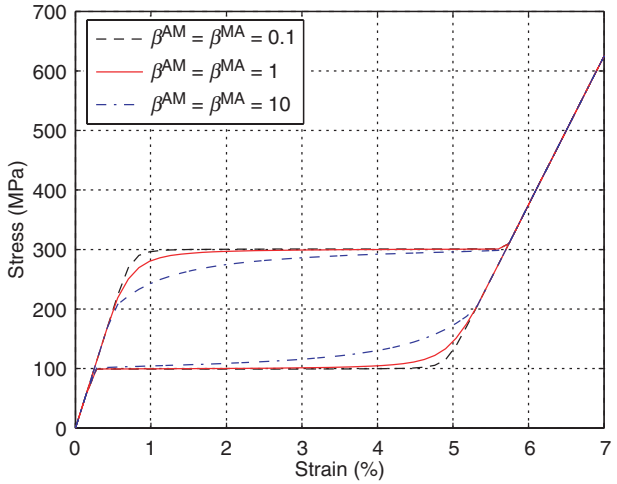

Figure 3. *Exponential rules: stress–strain relationship for quasi-static loading–unloading conditions.*

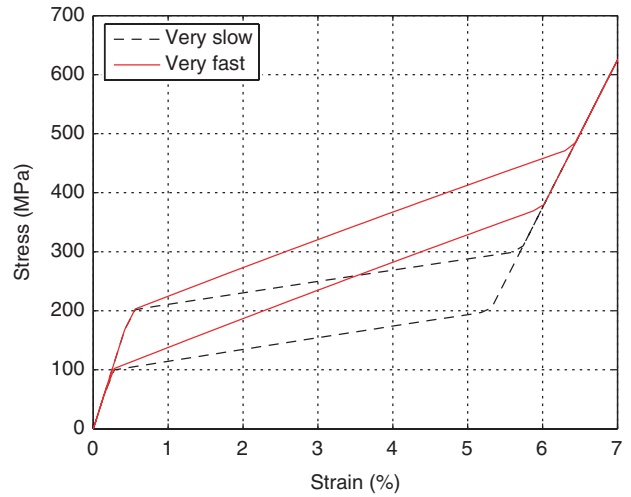

Figure 4. *Linear rules: stress–strain relationship for very slow and very fast loading–unloading conditions.*

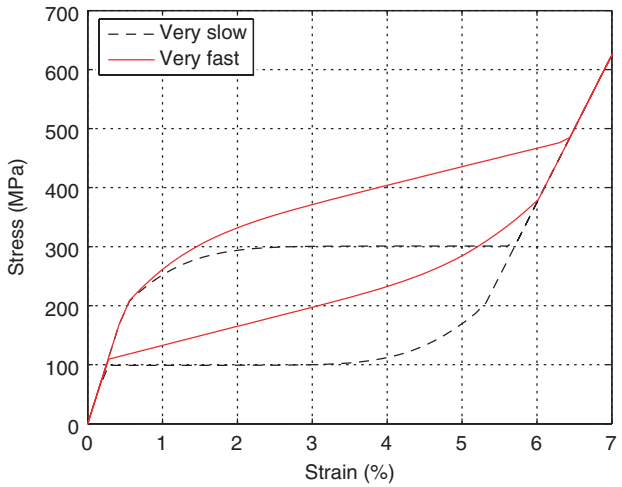

Figure 5. *Power rules: stress–strain relationship for very slow and very fast loading–unloading conditions ($\pi^{AM} = \pi^{MA} = 0.1$).*

Results from Test 1 are reported in Figures 2 and 3 in terms of stress–strain relationships and for the three considered kinetic rules. From their examination, we may draw the following conclusions.

- The linear rules (Figure 2) describe the superelastic effect by linearly connecting the corresponding start and finish phase transformation stress levels, therefore without reproducing the typical smooth behavior displayed by most SMAs.
- The power rules (Figure 2) show different behaviors according to the values of the speed parameters (i.e., π^{AM} and π^{MA}). In particular, if the π's are below or above 1, we observe a convexity change in the curves modelling the superelastic plateaus. Furthermore, if the π's are below 1 the stress–strain relationship does not seem to be realistic. Finally, it is possible to reproduce a linear kinetic upon setting $\pi^{AM} = \pi^{MA} = 1$.
- The exponential rules (Figure 3) show different behaviors according to the values of the speed parameters (i.e., β^{AM} and β^{MA}). Again, by properly choosing the β's, it would be possible to control the speed of the phase transition saturation.

Results from Test 2 are reported in Figures 4–6 and are still expressed in terms of stress–strain relationships for the three proposed kinetic rules. From their examination, we may draw the following conclusions.

- All kinetic rules are able to reproduce the experimentally observed (Dolce and Cardone, 2001; DesRoches

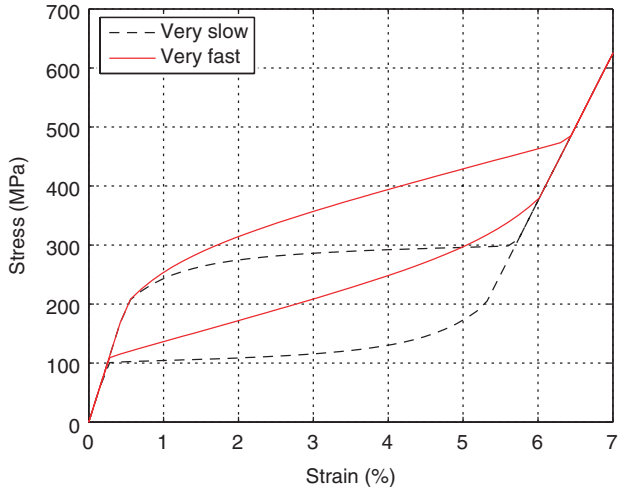

Figure 6. *Exponential rules: stress–strain relationship for very slow and very fast loading–unloading conditions ($\beta^{AM} = \beta^{MA} = 10$).*

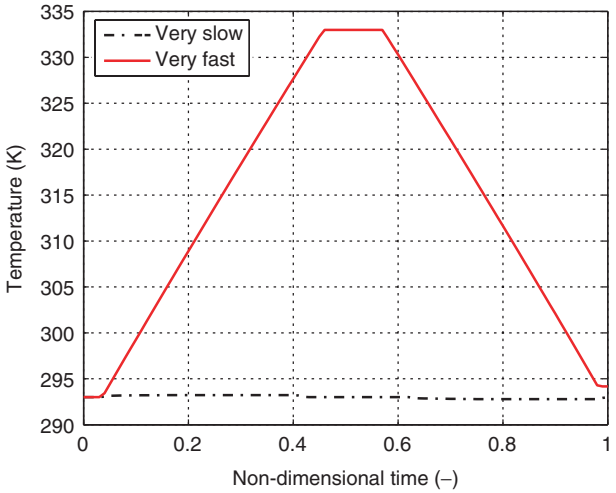

Figure 7. *Linear rules: evolution of the material temperature for very slow and very fast loading–unloading conditions.*

et al., 2004; Fugazza, 2005) increase of the stress levels at which the forward and reverse transformation finishes and starts, respectively, as the strain-rate increases.

- Linear, power, and exponential rules are all able to simulate the hysteresis size reduction with the increase of the strain-rate (Dolce and Cardone, 2001; DesRoches et al., 2004; Fugazza, 2005). Furthermore, by properly setting the speed parameters (i.e., π's and β's), it would be possible to model a wide range of superelastic behaviors (i.e., different responses of the material for the same loading–unloading pattern).
- Finally, in Figure 7, we observe the evolution of the material temperature during the deformation process. Its variation is negligible when performing quasi-static tests but it is not when considering high strain-rates. On the x-axis we represent the non-dimensional time (contained in the range [0, 1] for both simulations), with the aim of better comparing the model responses. For brevity, we only present the results related to the linear rules.

EXPERIMENTAL INVESTIGATION

We now want to test the ability of the model to simulate experimental data. We do this by comparing the numerical response with available experimental data related to superlastic SMA wires and bars provided by different suppliers.[3]

These are obtained from uniaxial tests consisting of multiple strain-driven loading–unloading cycles performed on virgin materials, at frequency levels of excitation typical of applications in earthquake engineering (Dolce and Cardone, 2001; DesRoches et al., 2004; Fugazza, 2005) and at room temperature (≈20°C). For simplicity, we only concentrate on a single cycle up to a 6% strain.

We consider three sets of experiments:

- *Set* 1: The material is a commercial superelastic NiTi straight wire with circular cross section of diameter 1.00 mm provided by CNR-IENI (Lecco, Italy). The testing frequencies were 0.001 Hz (quasi-static) and 1 Hz (dynamic).
- *Set* 2: The material is a commercial superelastic NiTi straight wire with circular cross section of diameter 0.76 mm provided by Memry Corp. (Menlo Park, USA). The testing frequencies were 0.001 Hz (quasi-static) and 0.1 Hz (dynamic).
- *Set* 3: The material is a commercial superelastic NiTi bar with circular cross section of diameter 12.7 mm provided by Special Metals Corporation (New Hartford, USA). The testing frequencies were 0.0025 Hz (quasi-static) and 1 Hz (dynamic).

Tests relative to the first two sets were performed by Fugazza (2005) at the Parco Scientifico Tecnologico e delle Telecomunicazioni in Valle Scrivia (Tortona, Italy), while tests considered in Set 3 were performed by DesRoches et al. (2004) at the Georgia Institute of Technology (Atlanta, USA). Both experimental studies

[3]The SMA materials were made of NiTi alloys whose chemical composition was not known. Also, no information regarding differential scanning calorimetry data and temperatures for the stress-free martensitic transformations was available.

Table 4. Mechanical properties of the considered SMA elements (L = linear rules, P = power rules, and E = exponential rules).

		Set 1			Set 2			Set 3		
		L	P	E	L	P	E	L	P	E
E_A	(MPa)	31000	31000	31000	61000	61000	61000	28500	28500	28500
E_M	(MPa)	24600	24600	24600	30000	30000	30000	24000	24000	24000
ϵ_L	(%)	4.10	4.10	4.10	4.80	4.80	4.80	2.90	2.90	2.90
σ_s^{AM}	(MPa)	310	200	200	350	350	350	270	210	210
σ_f^{AM}	(MPa)	370	370	370	370	370	370	530	530	530
σ_s^{MA}	(MPa)	60	250	250	150	250	250	350	420	490
σ_f^{MA}	(MPa)	35	35	35	135	135	135	90	90	90
π^{AM}	(–)	–	0.08	–	–	1.5	–	–	0.70	–
π^{MA}	(–)	–	0.12	–	–	0.1	–	–	0.75	–
β^{AM}	(–)	–	–	6.0	–	–	15.0	–	–	150
β^{MA}	(–)	–	–	9.8	–	–	4.0	–	–	120

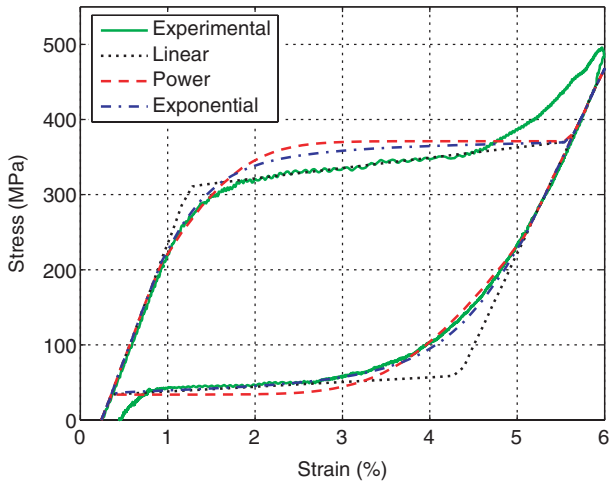

Figure 8. *Quasi-static loading conditions: experimental data (set 1) vs numerical results.*

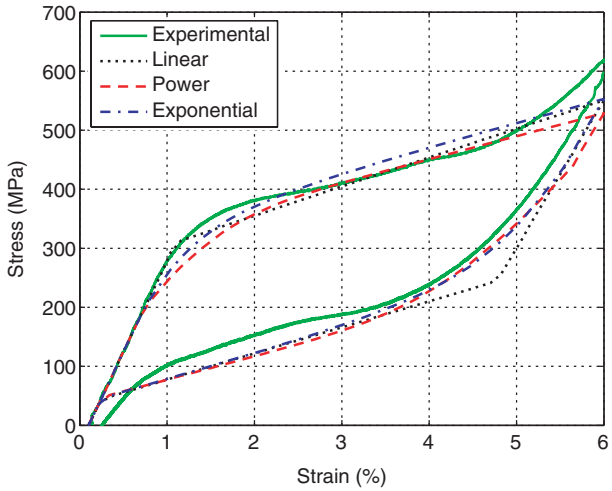

Figure 9. *Dynamic loading conditions: experimental data (set 1) vs numerical results.*

were aimed at investigating the cyclic properties of SMA wires and bars for seismic applications. Details regarding the testing equipment such as characteristics of the testing apparatus, software interface, extensometers used etc., can be found in the aforementioned references.

Besides the development of the constitutive model and its algorithmic implementation, the other goal of this study is to try to reproduce the rate-dependent superelastic behavior of the considered SMA elements. In particular, for each set of data we need to:

1. Obtain mechanical parameters E_A, E_M, ϵ_L common to all experimental curves belonging to the same set.
2. Obtain mechanical parameters σ_s^{AM}, σ_f^{AM}, σ_s^{MA}, and σ_f^{MA} from experimental tests performed at the lowest frequency. These data may vary according to the considered kinetic rules.
3. Obtain thermodynamic parameters Δu, $\Delta\eta$, C, α, and γ.
4. Find values of π^{AM} and π^{MA}, when considering power rules, and values of β^{AM} and β^{MA}, when considering exponential rules, in such a way to best fit the experimental curve obtained under quasi-static loading conditions.
5. Run numerical simulations for all strain-rates considered using the same material parameters throughout the analyses.
6. Compare experimental data and numerical results.

Mechanical properties of the considered SMA elements are summarized in Table 4 while thermodynamic parameters, which were not determined experimentally, are the same as those used in the previous section (i.e., Numerical Examples).

Comparison with Experimental Data

After performing the experimental tests, we now want to simulate them using the proposed model. In the following, we list and discuss the most important results.

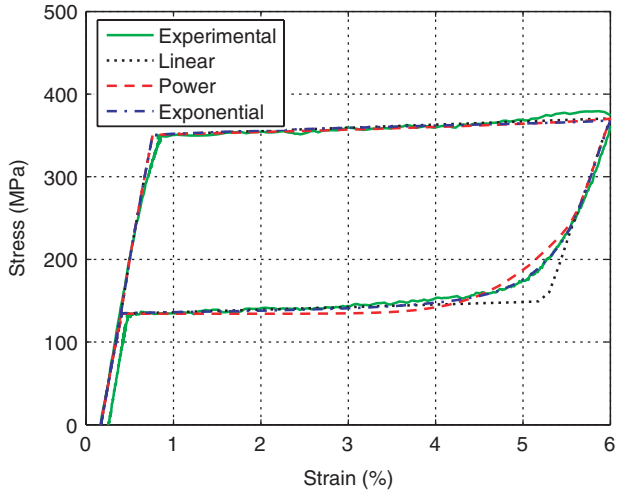

Figure 10. *Quasi-static loading conditions: experimental data (set 2) vs numerical results.*

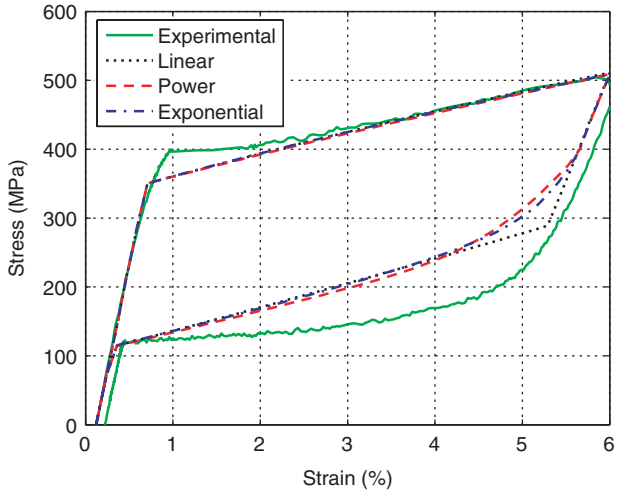

Figure 11. *Dynamic loading conditions: experimental data (set 2) vs numerical results.*

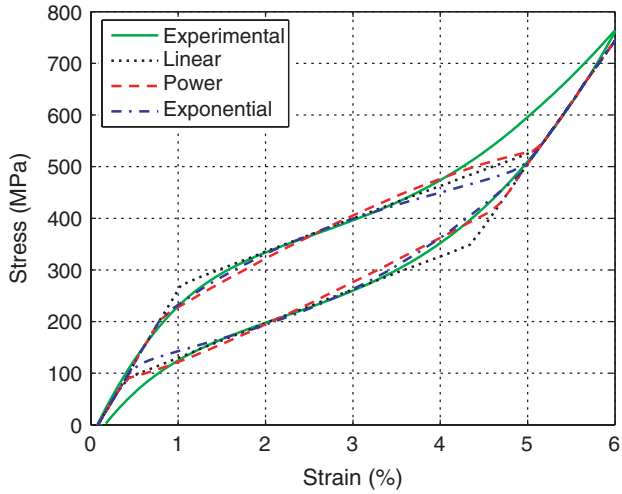

Figure 12. *Quasi-static loading conditions: experimental data (set 3) vs numerical results.*

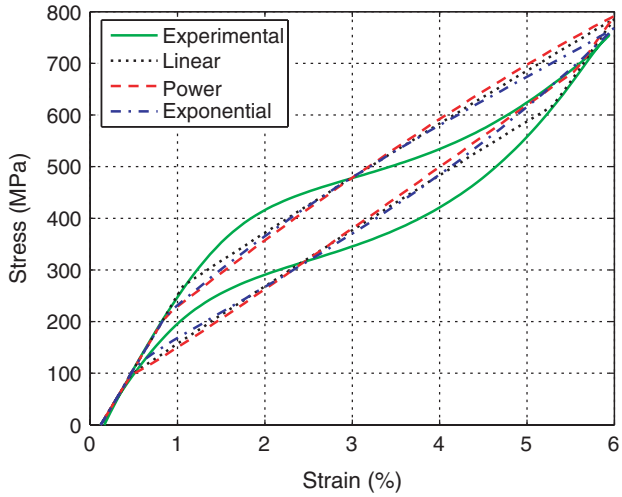

Figure 13. *Dynamic loading conditions: experimental data (set 3) vs numerical results.*

- From the quasi-static tests (Figures 8, 10, and 12), we observe a good match between experiments and numerical results, specially when power and exponential rules are used to model the evolution of the martensite fraction during the deformation process. However, as it is clear from the comparison related to the Memry wires (set 2), the model is unable to simulate the stress drop seen at the beginning of the forward transformation, which is a clear sign of Lüders-band effects (Liu et al., 1998).
- When exploiting the dynamic conditions, we note that the ability of the model to reproduce experimental data strongly depends on the type of SMA material under investigation. More precisely, when we consider the first set of data (Figure 9) we observe a very good fit of the model response with the experimental curve. On the other hand, we do not observe the same trend for the second and third set of data (Figures 11 and 13) where, however, the model provides a good estimate of the stress value reached at the maximum strain level being considered. Such a discrepancy could be justified by the fact that the heat flux has been neglected in the constitutive modelling. As a consequence, the hypothesis of uniform temperature field inside the material leads to better results when considering the wires which are characterized by smaller cross sectional sizes than the bars.
- The model successfully simulates complete transformation patterns by correctly capturing the material hardening (i.e., fully martensitic phase) observed at the end of the upper superelastic plateau (Figures 8 and 12).

- Despite the fact that chemical composition, thermomechanical treatments and manufacturing processes may result in showing a different material behavior under the same loading conditions, the capability of the model to describe the hysteresis size reduction at high frequency levels is always noticed.

CONCLUSIONS

In this article, we proposed a uniaxial thermomechanical constitutive model able to reproduce the rate-dependent superelastic effect exhibited by SMAs and able to take into account the different elastic properties between austenite and martensite.

In the following, we summarize the major outcomes based on the numerical tests as well as on the comparisons with the experimental data.

- The model is based on a single scalar internal variable, the martensite fraction, for which three different rate-independent evolutionary equations written in rate form are presented.
- The coupling of the rate-independent kinetic rules with the heat equation allows for the modelling of the SMAs' rate-dependent behavior through the simulation of the material temperature time-history during the loading action.
- The model requires a limited number of mechanical parameters which can be obtained from typical uniaxial tests. They are the Young's modulus of austenite and martensite, the plateau length and the stress levels at which the phase transformations take place. On the other hand, the thermodynamic parameters are not straightforward to determine experimentally but can be easily found in the literature for typical SMAs.
- Both power and exponential evolutionary equations are able to simulate the smooth transition occurring between the pure elastic behavior (either austenite or martensite) and the superelastic plateaus, as experimental evidences display.
- The capacity of the model to simulate experimental data has also been assessed. In particular, quasi-static tests have provided a good comparison between experiments and numerical results meanwhile the dynamic tests were strongly affected by the different rate-dependent response (i.e., different material response exhibited by each SMA for the same loading frequency) of the SMA material under study, probably due to the different chemical composition.

In conclusion, the advantages of the presented model are the simplicity, the possibility of implementing a robust solution algorithm, and the ability to reproduce experimental data obtained at different frequency levels of excitation for seismic application purposes.

ACKNOWLEDGEMENTS

The second author of this article would like to thank Ms Federica Onano of Parco Scientifico Tecnologico e delle Telecomunicazioni in Valle Scrivia (Tortona, Italy) and Dr Lorenza Petrini of Politecnico di Milano (Milano, Italy) for their help during the experimental tests, the Italian National Civil Protection Department (Roma, Italy) which, through its Servizio Sismico Nazionale section, provided a scholarship as well as the financial support of Progetto Giovani Ricercatori - Anno 2002 of the Università degli Studi di Pavia (Pavia, Italy). Also, the funding of the Ministero dell'Istruzione, dell'Università e della Ricerca (MIUR) through the research programs 'Shape-memory alloys: constitutive modelling, structural analysis and design of innovative biomedical applications' and 'Shape-memory alloys: constitutive modelling, structural behavior, experimental validation and applicability to innovative biomedical applications' is kindly acknowledged. Additional funding was provided by the PECASE Program of the National Science Foundation under Grant No. 0093868.

APPENDIX 1

Linear Kinetic Rules

CONVERSION OF AUSTENITE INTO MARTENSITE

$$C_2 = (E_A - E_M)(F_n - R_f^{AM})$$

$$C_1 = E_A E_M \epsilon_L (\xi_n - 1) + E_M (F_n - R_f^{AM}) + (E_A - E_M)\left[A(\xi_n - 1)(T - T_U) - F_n + \xi_n R_f^{AM}\right]$$

$$C_0 = -E_A E_M \epsilon \,\mathrm{sgn}(\epsilon)(\xi_n - 1) + E_M\left[A(\xi_n - 1)(T - T_U) - F_n + \xi_n R_f^{AM}\right].$$

CONVERSION OF MARTENSITE INTO AUSTENITE

$$C_2 = (E_A - E_M)(F_n - R_f^{MA})$$

$$C_1 = E_A E_M \epsilon_L \xi_n + E_M (F_n - R_f^{MA}) + (E_A - E_M)\left[A\xi_n (T - T_U) + \xi_n R_f^{MA}\right]$$

$$C_0 = -E_A E_M \epsilon \,\mathrm{sgn}(\epsilon)\xi_n + E_M \xi_n\left[A(T - T_U) + R_f^{MA}\right].$$

Power Kinetic Rules

CONVERSION OF AUSTENITE INTO MARTENSITE

$$C_2 = E_A E_M \epsilon_L (\pi^{AM} - 1) + (E_A - E_M)\left[A(T - T_U)(\pi^{AM} - 1) + \pi^{AM} F_n - R_f^{AM}\right]$$

$$C_1 = E_A E_M \epsilon \,\mathrm{sgn}(\epsilon)(1 - \pi^{AM}) + E_A E_M \epsilon_L (\xi_n - \pi^{AM}) + E_M(\pi^{AM} F_n - R_f^{AM}) - A E_M (T - T_U)(1 - \pi^{AM}) + (E_A - E_M)\left[A(\xi_n - \pi^{AM})(T - T_U) - \pi^{AM} F_n + \xi_n R_f^{AM}\right]$$

$$C_0 = -E_A E_M \epsilon \,\mathrm{sgn}(\epsilon)(\xi_n - \pi^{AM}) + E_M\left[A(\xi_n - \pi^{AM})(T - T_U) - \pi^{AM} F_n + \xi_n R_f^{AM}\right].$$

CONVERSION OF MARTENSITE INTO AUSTENITE

$$C_2 = E_A E_M \epsilon_L (\pi^{MA} - 1) + (E_A - E_M)\left[A(T - T_U)(\pi^{MA} - 1) + \pi^{MA} F_n - R_f^{MA}\right]$$

$$C_1 = E_A E_M \epsilon \,\mathrm{sgn}(\epsilon)(1 - \pi^{MA}) + E_A E_M \epsilon_L \xi_n + E_M(\pi^{MA} F_n - R_f^{MA}) - A E_M (T - T_U)(1 - \pi^{MA}) + (E_A - E_M)\left[A\xi_n (T - T_U) + \xi_n R_f^{MA}\right]$$

$$C_0 = -E_A E_M \epsilon \,\mathrm{sgn}(\epsilon)\xi_n + E_M \xi_n \left[A(T - T_U) + R_f^{MA}\right].$$

Exponential Kinetic Rules

CONVERSION OF AUSTENITE INTO MARTENSITE

$$C_3 = (E_A E_M \epsilon_L)^2 + (E_A - E_M)^2 \times \left\{\left[A(T - T_U) + R_f^{AM}\right]^2 - \beta^{AM}[A(T - T_U) + F_n]\right\} + E_A E_M (E_A - E_M)\epsilon_L \left\{2\left[A(T - T_U) + R_f^{AM}\right] - \beta^{AM}\right\}$$

$$C_2 = (E_A E_M)^2 \left\{-\epsilon_L[2\epsilon \,\mathrm{sgn}(\epsilon) + \xi_n \epsilon_L]\right\} + 2E_M(E_A - E_M) \times \left\{\left[A(T - T_U) + R_f^{AM}\right]^2 - \beta^{AM}[A(T - T_U) + F_n]\right\} + E_A E_M (E_A - E_M)\left\{-2A(T - T_U)[\epsilon \,\mathrm{sgn}(\epsilon) + \xi_n \epsilon_L] + \epsilon \,\mathrm{sgn}(\epsilon)\left[\beta^{AM} - 2R_f^{AM}\right] - \epsilon_L\left[\beta^{AM} - 2\xi_n R_f^{AM}\right]\right\} - (E_A E_M)^2 \left\{\xi_n\left[A(T - T_U) + R_f^{AM}\right]^2 - \beta^{AM}[A(T - T_U) + F_n] + E_A E_M^2 \epsilon_L \left\{2\left[A(T - T_U) + R_f^{AM}\right] - \beta^{AM}\right\}\right.$$

$$C_1 = (E_A E_M)^2 \epsilon \left\{[\epsilon + 2\xi_n \epsilon_L \,\mathrm{sgn}(\epsilon)]\right\} + E_M^2 \left\{\left[A(T - T_U) + R_f^{AM}\right]^2 - \beta^{AM}[A(T - T_U) + F_n]\right\} + E_A E_M (E_A - E_M)\epsilon \,\mathrm{sgn}(\epsilon) \times \left\{2\xi_n\left[A(T - T_U) + R_f^{AM}\right] - \beta^{AM}\right\} - E_M(E_A - E_M)\left\{2\xi_n\left[A(T - T_U) + R_f^{AM}\right]^2 - 2\beta^{AM}[A(T - T_U) + F_n]\right\} - E_A E_M^2 \left\{2A(T - T_U)[\epsilon \,\mathrm{sgn}(\epsilon) + \xi_n \epsilon_L] + \epsilon \,\mathrm{sgn}(\epsilon)\left[2R_f^{AM} - \beta^{AM}\right] + \epsilon_L\left[2\xi_n R_f^{AM} - \beta^{AM}\right]\right\}$$

$$C_0 = -\xi_n (E_A E_M \epsilon)^2 - E_M^2 \left\{\xi_n\left[A(T - T_U) + R_f^{AM}\right]^2 - \beta^{AM}[A(T - T_U) + F_n]\right\} + E_A E_M^2 \epsilon \,\mathrm{sgn}(\epsilon)\left\{2\xi_n\left[A(T - T_U) + R_f^{AM}\right] - \beta^{AM}\right\}.$$

CONVERSION OF MARTENSITE INTO AUSTENITE

$$C_3 = (E_A E_M \epsilon_L)^2 + (E_A - E_M)^2 \times \left\{\left[A(T - T_U) + R_f^{MA}\right]^2 + \beta^{MA}[A(T - T_U) + F_n]\right\} + E_A E_M (E_A - E_M)\epsilon_L \times \left\{2\left[A(T - T_U) + R_f^{MA}\right] + \beta^{MA}\right\}$$

$$
\begin{aligned}
C_2 = {} & (E_A E_M)^2 \left\{ -\epsilon_L [2\epsilon \operatorname{sgn}(\epsilon) + \xi_n \epsilon_L] \right\} \\
& + 2 E_M (E_A - E_M) \left\{ \left[A(T - T_U) + R_f^{MA} \right]^2 \right. \\
& \left. + \beta^{MA} [A(T - T_U) + F_n] \right\} + E_A E_M (E_A - E_M) \\
& \times \left\{ -2A(T - T_U)[\epsilon \operatorname{sgn}(\epsilon) + \xi_n \epsilon_L] \right. \\
& \left. - \epsilon \operatorname{sgn}(\epsilon) \left[\beta^{MA} + 2 R_f^{MA} \right] - 2 \epsilon_L \xi_n R_f^{MA} \right\} \\
& - (E_A E_M)^2 \xi_n \left[A(T - T_U) + R_f^{MA} \right]^2 \\
& + E_A E_M^2 \epsilon_L \left\{ 2 \left[A(T - T_U) + R_f^{MA} \right] + \beta^{MA} \right\} \\
C_1 = {} & (E_A E_M)^2 \epsilon \left\{ [\epsilon + 2 \xi_n \epsilon_L \operatorname{sgn}(\epsilon)] \right\} \\
& + E_M^2 \left\{ \left[A(T - T_U) + R_f^{MA} \right]^2 \right. \\
& \left. + \beta^{MA} [A(T - T_U) + F_n] \right\} \\
& + 2 \xi_n E_A E_M (E_A - E_M) \epsilon \operatorname{sgn}(\epsilon) \\
& \times \left[A(T - T_U) + R_f^{MA} \right] \\
& + 2 \xi_n E_M (E_A - E_M) \left[A(T - T_U) + R_f^{MA} \right]^2 \\
& - E_A E_M^2 \left\{ 2 A(T - T_U)[\epsilon \operatorname{sgn}(\epsilon) + \xi_n \epsilon_L] \right. \\
& \left. + \epsilon \operatorname{sgn}(\epsilon) \left[2 R_f^{MA} + \beta^{MA} \right] + 2 \xi_n R_f^{MA} \epsilon_L \right\} \\
C_0 = {} & -\xi_n (E_A E_M \epsilon)^2 - E_M^2 \left\{ \xi_n \left[A(T - T_U) + R_f^{MA} \right]^2 \right. \\
& \left. + 2 E_A E_M^2 \epsilon \operatorname{sgn}(\epsilon) \xi_n \left[A(T - T_U) + R_f^{MA} \right] \right\}.
\end{aligned}
$$

REFERENCES

Anand, L. and Gurtin, M.E. 2003. "Thermal Effects in the Superelasticity of Crystalline Shape-memory Materials," *Journal of the Mechanics and Physics of Solids*, 5(6):1015–1058.

Auricchio, F. 1995. "Shape-memory Alloys: Applications, Micromechanics, Macromodelling and Numerical Simulations," PhD Thesis, Department of Civil Engineering, University of California at Berkeley.

Auricchio, F., Fugazza, D. and DesRoches, R. 2006. "A 1D Rate-dependent Constitutive Model for Superelastic Shape-memory Alloys: Formulation and Comparison with Experimental Data," *Smart Materials and Structures* (in press).

Auricchio, F. and Sacco, E. 1997. "A One-dimensional Model for Superelastic Shape-memory Alloys with Different Elastic Properties Between Austenite and Martensite," *International Journal of Non-Linear Mechanics*, 32(6):1101–1114.

Auricchio, F. and Sacco, E. 1999a. "Modelling of the Rate-dependent Superelastic Behavior of Shape-memory Alloys," In *ECCM 99, European Conference on Computational Mechanics*, August 31–September 3, München, Germany.

Auricchio, F. and Sacco, E. 1999b. "A Temperature-dependent Beam For Shape-memory Alloys: Constitutive Modelling, Finite-element Implementation and Numerical Simulations," *Computer Methods in Applied Mechanics and Engineering*, 174(1–2):171–190.

Auricchio, F. and Sacco E. 2001. "Thermo-mechanical Modelling of a Superelastic Shape-memory Wire Under Cyclic Stretching–Bending Loadings," *International Journal of Solids and Structures*, 38(34–35):6123–6145.

Bernardini, D. and Brancaleoni, F. 1999. "Shape Memory Alloys Modelling for Seismic Applications," *Atti del MANSIDE Project - Final Workshop - Memory Alloys for New Seismic Isolation and Energy Dissipation Devices*, 73–84.

Bernardini, D. and Pence, T.J. 2002. "Models for One-variant Shape Memory Materials Based on Dissipation Functions," *International Journal of Non-Linear Mechanics*, 37(8):1299–1317.

Brinson, L.C., Schmidt, I. and Lammering, R. 2004. "Stress-induced Transformation Behavior of a Polycrystalline NiTi Shape Memory Alloy: Micro and Macromechanical Investigations Via In Situ Optical Microscopy," *Journal of the Mechanics and Physics of Solids*, 52(7):1549–1571.

DesRoches, R., McCormick, J. and Delemont, M. 2004. "Cyclic Properties of Superelastic Shape Memory Alloy Wires and Bars," *Journal of Structural Engineering*, 130(1):38–46.

DesRoches, R. and Smith, B. 2004. "Shape Memory Alloys in Seismic Resistant Design and Retrofit: A Critical Review of Their Potential and Limitations," *Journal of Earthquake Engineering*, 8(3):415–429.

Dolce, M. and Cardone, D. 2001. "Mechanical Behaviour of Shape Memory Alloys for Seismic Applications 2. Austenite NiTi Wires Subjected to Tension," *International Journal of Mechanical Sciences*, 43(11):2657–2677.

Duerig, T.W., Melton, K.N., Stokel, D. and Wayman, C.M. 1990. *Engineering Aspects of Shape Memory Alloys*. Butterworth-Henemann, London.

Entemeyer, D., Patoor, E., Eberhardt, A. and Berveiller, M. 2000. "Strain Rate Sensitivity in Superelasticity," *International Journal of Plasticity*, 16(10–11):1268–1288.

Fugazza, D. 2005. "Experimental Investigation on the Cyclic Properties of Superelastic NiTi Shape-memory Alloy Wires and Bars," *Individual study, European School for Advanced Studies in Reduction of Seismic Risk* (ROSE School), Pavia, Italy.

Graesser, E.J. and Cozzarelli, F.A. 1991. "Shape-memory Alloys as New Materials for Aseismic Isolation," *Journal of Engineering Mechanics*, 117(11):2590–2608.

Ikeda, T., Nae, F.A., Naito, H. and Matsuzaki, Y. 2004. "Constitutive Model of Shape Memory Alloys for Unidirectional Loading Considering Inner Hysteresis Loops," *Smart Materials and Structures*, 13(4):916–925.

Leclercq, S. and Lexcellent, C. 1996. "A general Macroscopic Description of the Thermomechanical Behavior of Shape Memory Alloys," *Journal of the Mechanics and Physics of Solids*, 44(6):953–980.

Lemaitre, J. and Chaboche, J. 1990. *Mechanics of Solid Materials*, Cambridge University Press, Cambridge, MA, USA.

Lim, T.J. and McDowell, D.L. 2002. "Cyclic Thermomechanical Behavior of a Polycrystalline Pseudoelastic Shape Memory Alloy," *Journal of the Mechanics and Physics of Solids*, 50(3):651–676.

Liu, Y., Liu, Y. and Humbeeck, J.V. 1998. "Lüders-like Deformation Associated With Martensite Reorientation in NiTi. *Scripta Materialia*, 39(8):1047–1055.

Lubliner, J. and Auricchio, F. 1996. "Generalized Plasticity and Shape Memory Alloys," *International Journal of Solids and Structures*, 33(7):991–1003.

Müller, I. and Seelecke, S. 2001. "Thermodynamic Aspects of Shape Memory Alloys," *Mathematical and Computer Modelling*, 34(12–13):1307–1355.

Saadat, S., Salichs, J., Noori, M., Hou, Z., Davoodi, H., Bar-on, I., Suzuki, Y. and Masuda, A. 2002. "An Overview of Vibration and Seismic Applications of NiTi Shape Memory Alloy," *Smart Materials and Structures*, 11(2):218–229.

Shaw, J.A. and Kyriakides, S. 1995. "Thermomechanical Aspects of NiTi," *Journal of the Mechanics and Physics of Solids*, 43(8):1243–1281.

Shaw, J.A. and Kyriakides, S. 1997. "On the Nucleation and Propagation of Phase Transformation Fronts in a NiTi Alloy," *Acta Materialia*, 45(2):683–700.

Tamai, H. and Kitagawa, Y. 2002. "Pseudoelastic Behavior of Shape Memory Alloy Wire and its Application to Seismic Resistance Member for Building," *Computational Materials Science*, 25(1–2):218–227.

Wilde, K., Gardoni, P. and Fujino, Y. 2000. "Base Isolation System with Shape Memory Alloy Device for Elevated Highway Bridges," *Engineering Structures*, 22(3):222–229.

Wilson, J. and Wesolowsky, M. 2005. "Shape Memory Alloys for Seismic Response Modification: A State-of-the-art Review," *Earthquake Spectra*, 21(2):569–601.